Supporting Information

Dipole Induced Rectification across Ag^{TS}/SAM//Ga_2O_3/EGaIn Junctions

*Mostafa Baghbanzadeh,[†] Lee Belding,[†] Li Yuan, Mohammad H. Al-Sayah, Carleen M. Bowers, and George M. Whitesides**

** To whom correspondence may be addressed: gwhitesides@gmwgroup.harvard.edu*

[†]Authors contributed equally to this work.

General Information

Materials. All organic solvents were analytical grade (99%, Sigma-Aldrich) and were used as supplied unless otherwise specified. Standard *n*-alkanethiolates were commercially available (≥ 98%, Sigma-Aldrich). The synthesis of Series I and Series II compounds is described below. All thiolate-based compounds were stored under a N_2 atmosphere and at < 4°C to avoid oxidation to the corresponding disulfide, sulfonate, or sulfonic acid. To ensure that the compounds were free of contaminants, all stored compounds were checked by ^{1}H NMR prior to use; any impurities were removed by silica gel column chromatography.

Charge Transport Measurements

Junction measurements using "selected" conical tips of EGaIn. We use EGaIn (eutectic Ga-In; 74.5% Ga, 25.5% In) as a non-damaging top electrode for measuring currents in junctions having the structure Ag^{TS}/SAM //Ga_2O_3/EGaIn.[1-2] This liquid metal forms a self-passivating oxide layer of Ga_2O_3 (0.7 nm thick on average) when exposed to air. We prepared EGaIn conical tips to use as the top contact, and selected tips that were free of visible surface asperities; conical tips that had visible irregularities (by optical microscopy) were not used.[3] We ensured that the contact area made between the tip and the SAM surface[4] was ≥ 1000 μm^2. Every junction (for which we collect 21 *J*(V) traces) was made with a newly prepared conical tip.

Measurement protocol. The SAMs were prepared on template stripped substrates[5] using thiol as the anchoring group according to protocols previously reported.[6-7] We measured between 12 and 17 junctions (individual points of contact between a Ga_2O_3/EGaIn tip and the SAM) for each compound investigated and collected about 21 *J*(V) traces for each junction. A *J*(V) trace involved sweeping from 0 V → +0.5 V → −0.5 V → 0 V in steps of 100 mV, with a delay of 0.2 s between each step in applied bias, while measuring *J* at each bias.

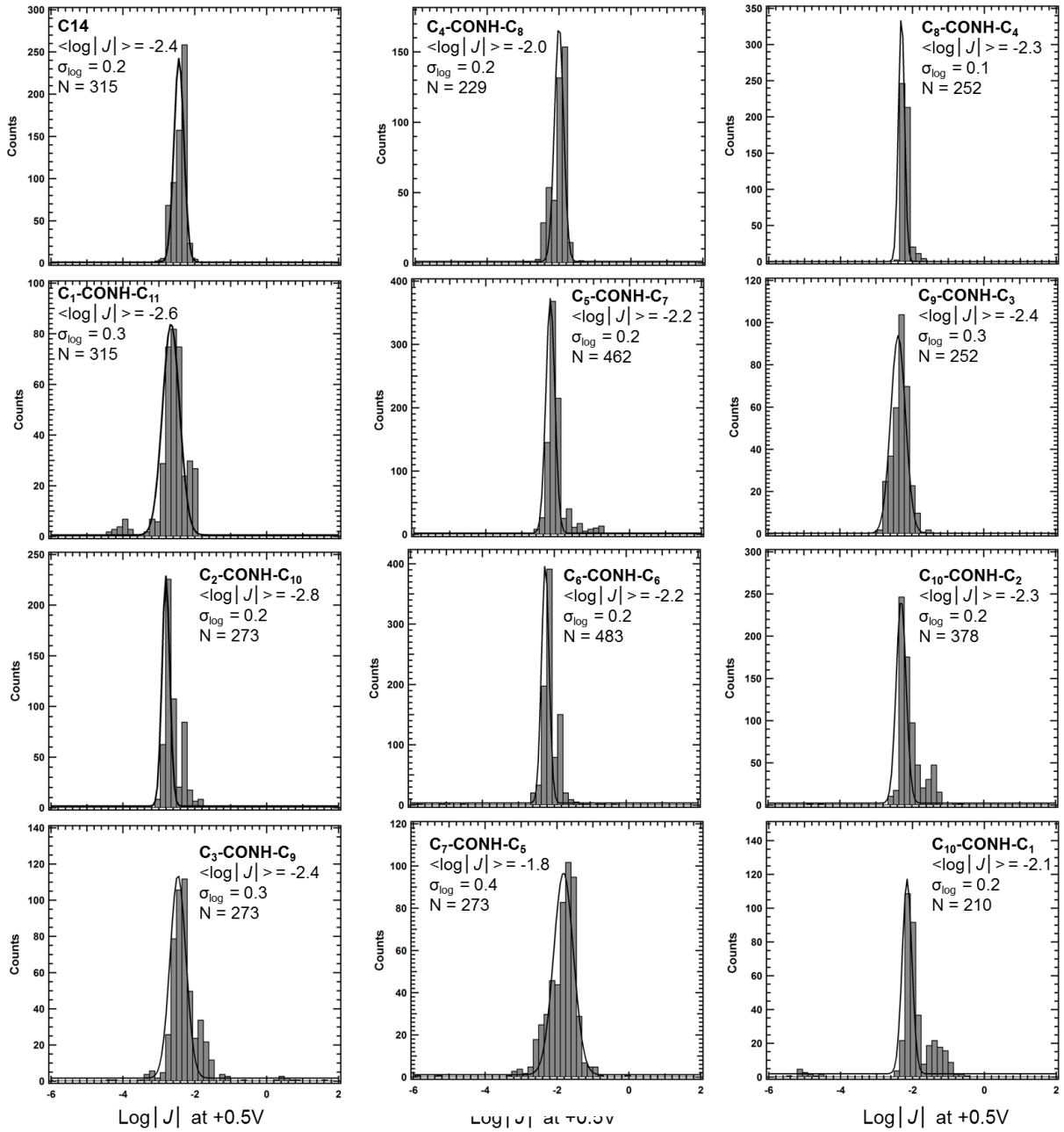

Figure S1. Histograms of current densities (at +0.5V) of Series I in Figure 1 (N: number of data; <log|*J*|>: population mean of log|*J*|; log|σ_J|: log scale of standard deviation of *J*).

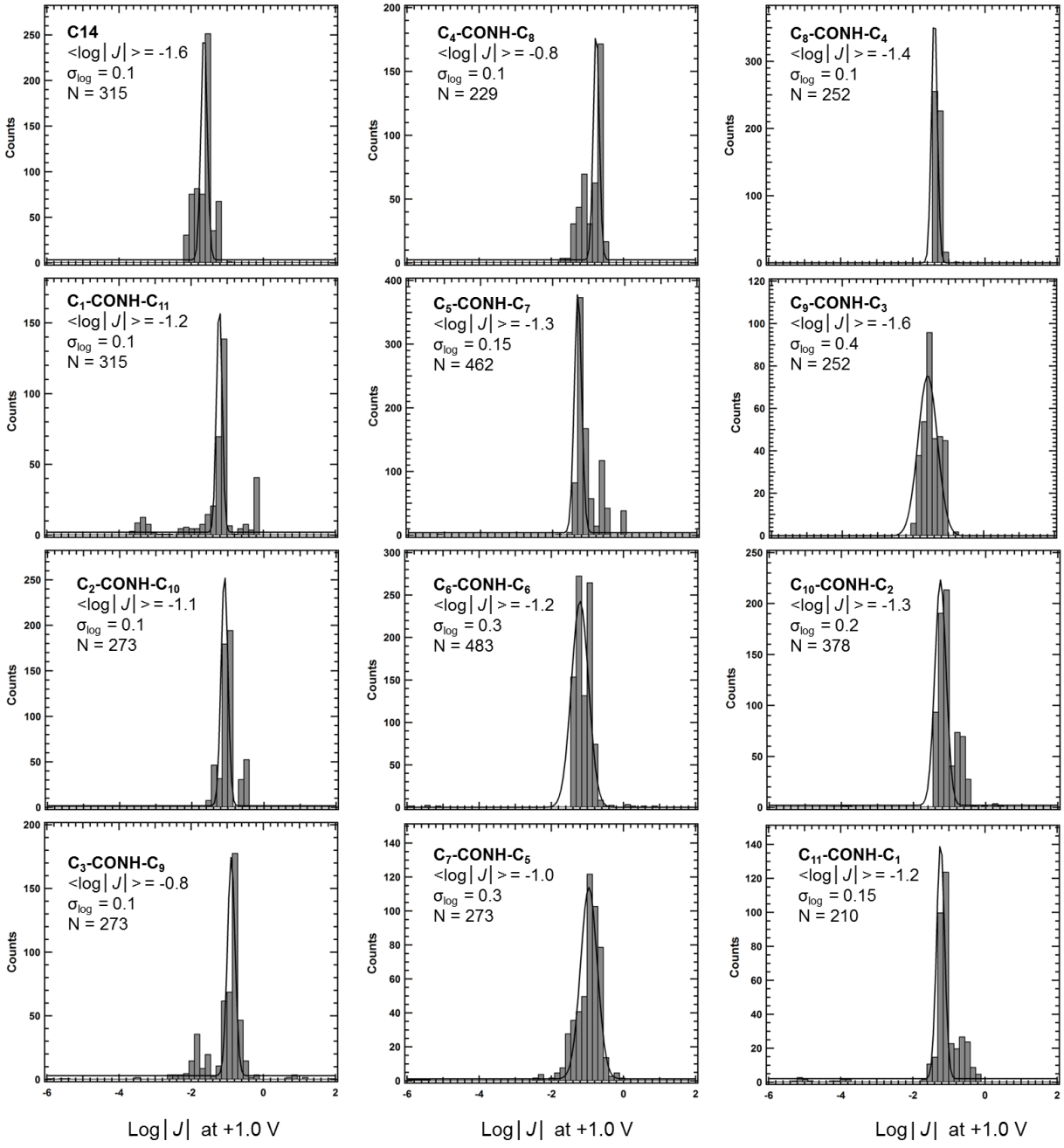

Figure S2. Histograms of current densities (at +1.0 V) of Series I in Figure 1 (N: number of data; <log|*J*|>: population mean of log|*J*|; log|σ_J|: log scale of standard deviation of *J*).

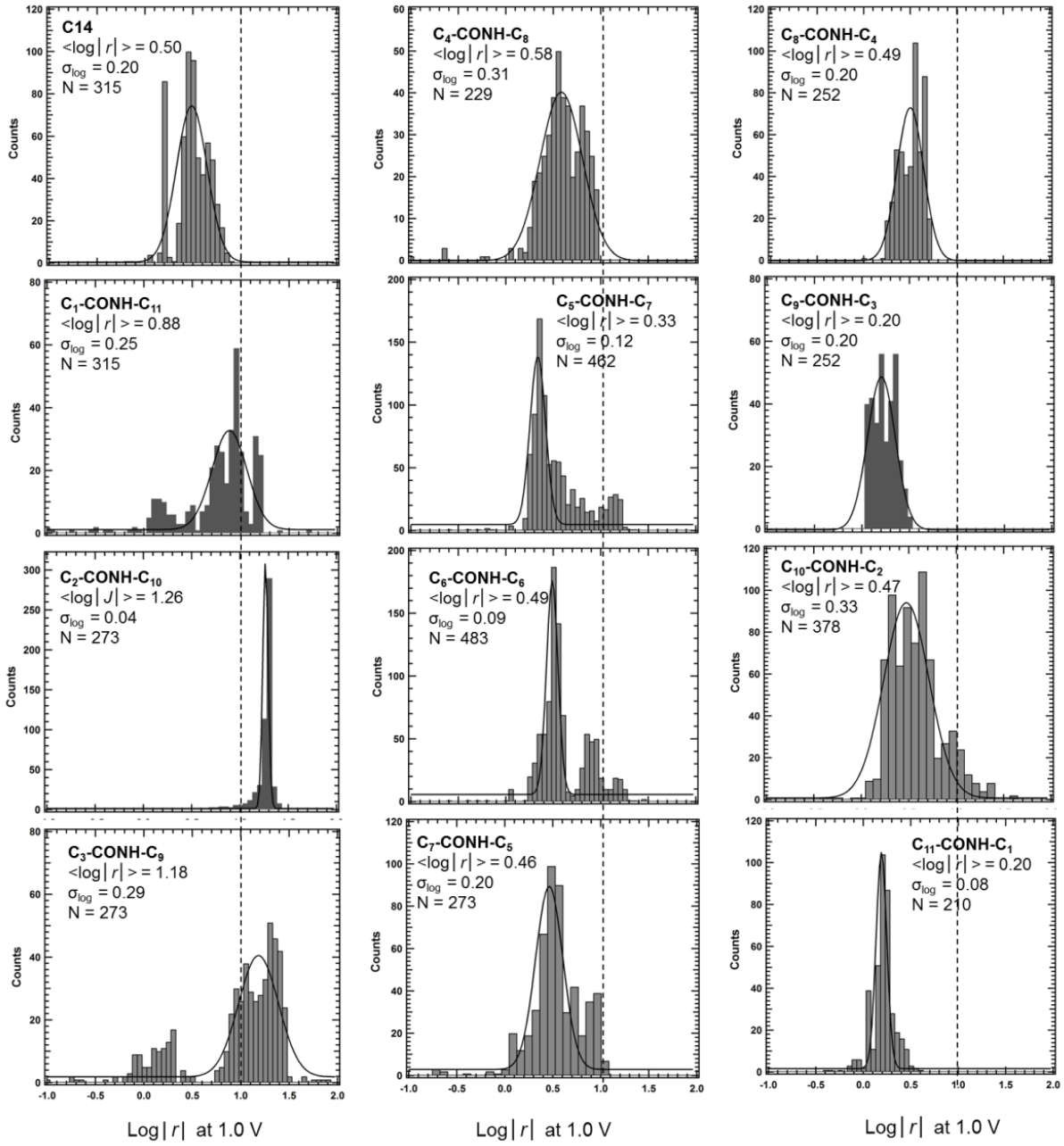

Figure S3. Histograms of the rectification ratio (r) at +1.0 V of series I derivatives in Figure 1 (N: number of data; r= <|J(+1.0 V)|/|J(-1.0 V)|>; σ: standard deviation of r).

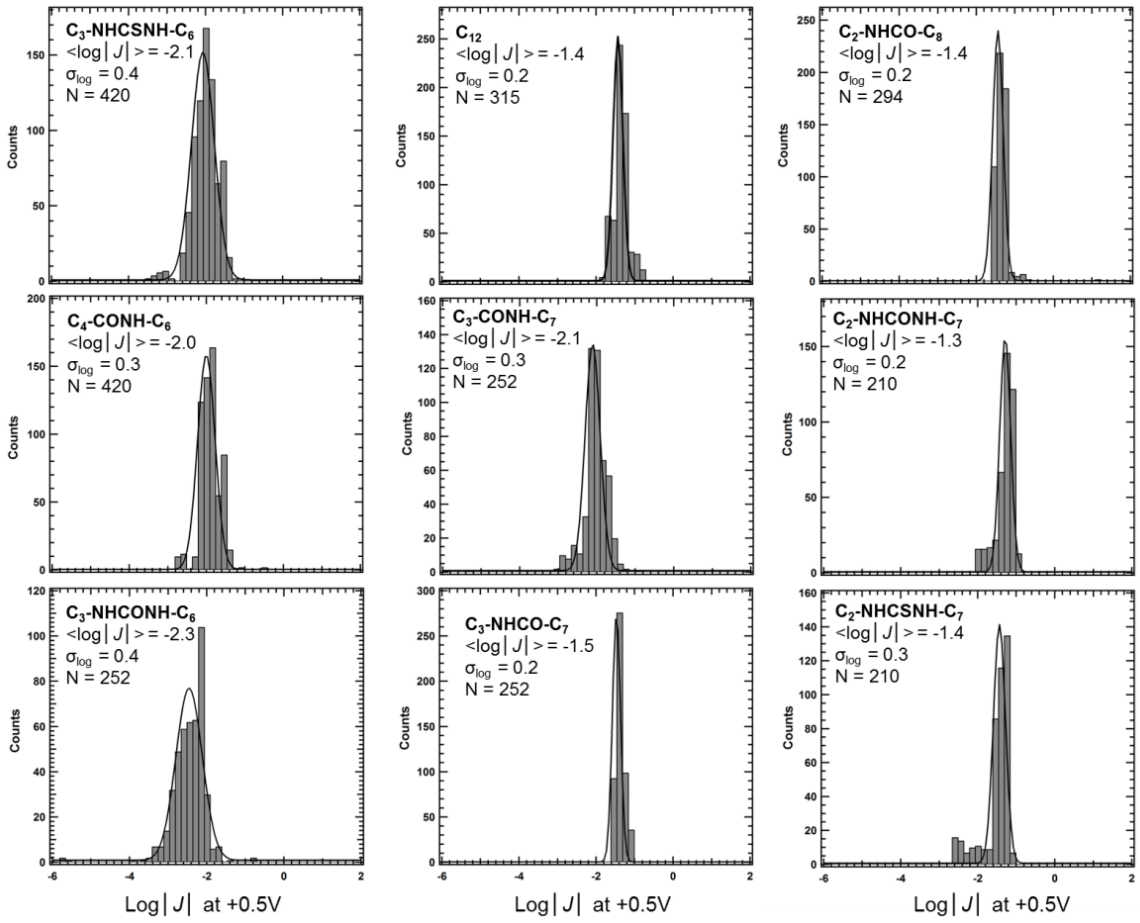

Figure S4. Histograms of current densities (at +0.5V) of Series II in Figure 1 (N: number of data; <log|*J*|>: population mean of log|*J*|; log|σ_J|: log scale of standard deviation of *J*).

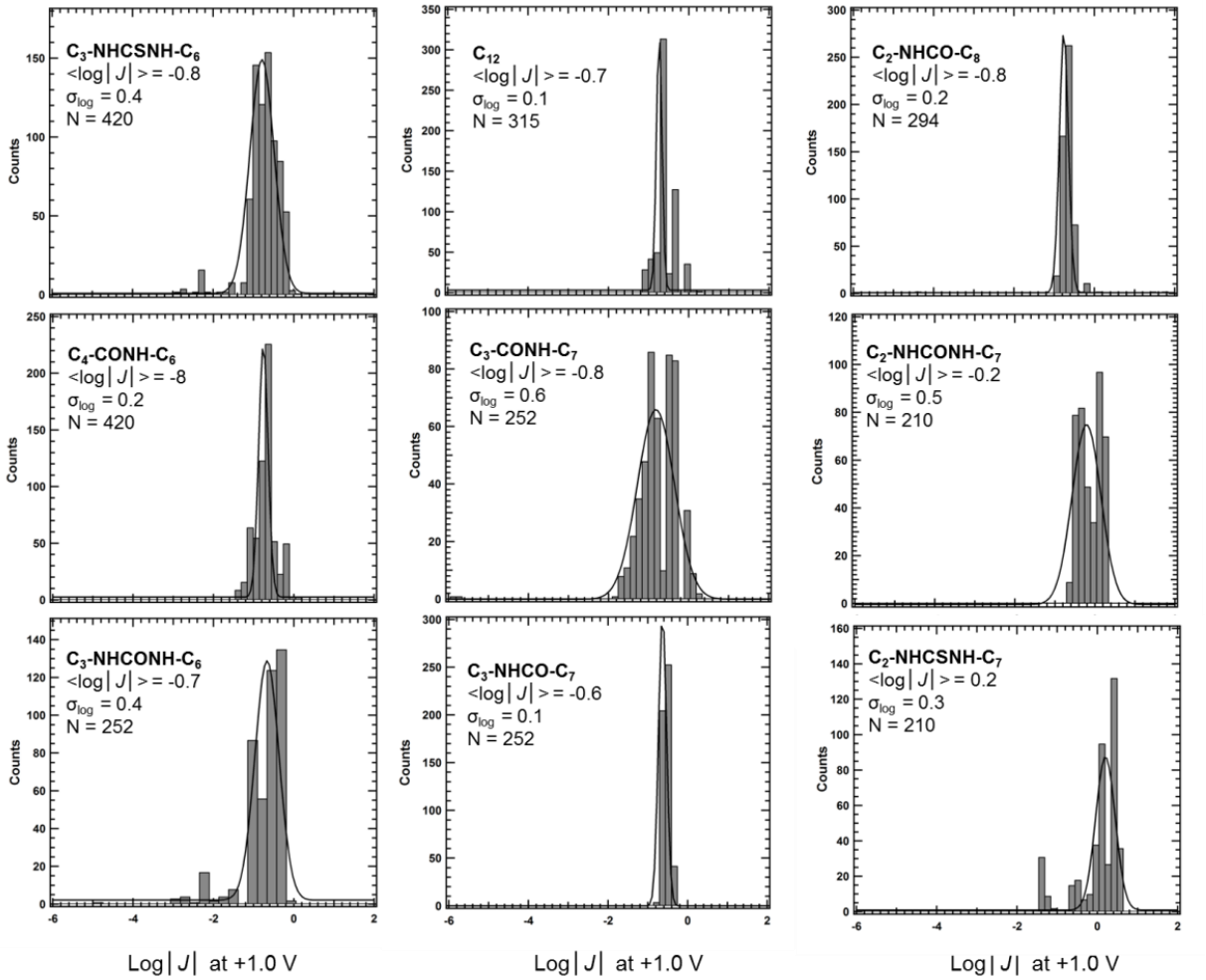

Figure S5. Histograms of current densities (at +1.0 V) of Series II in Figure 1 (N: number of data; <log|*J*|>: population mean of log|*J*|; log|σ_J|: log scale of standard deviation of *J*).

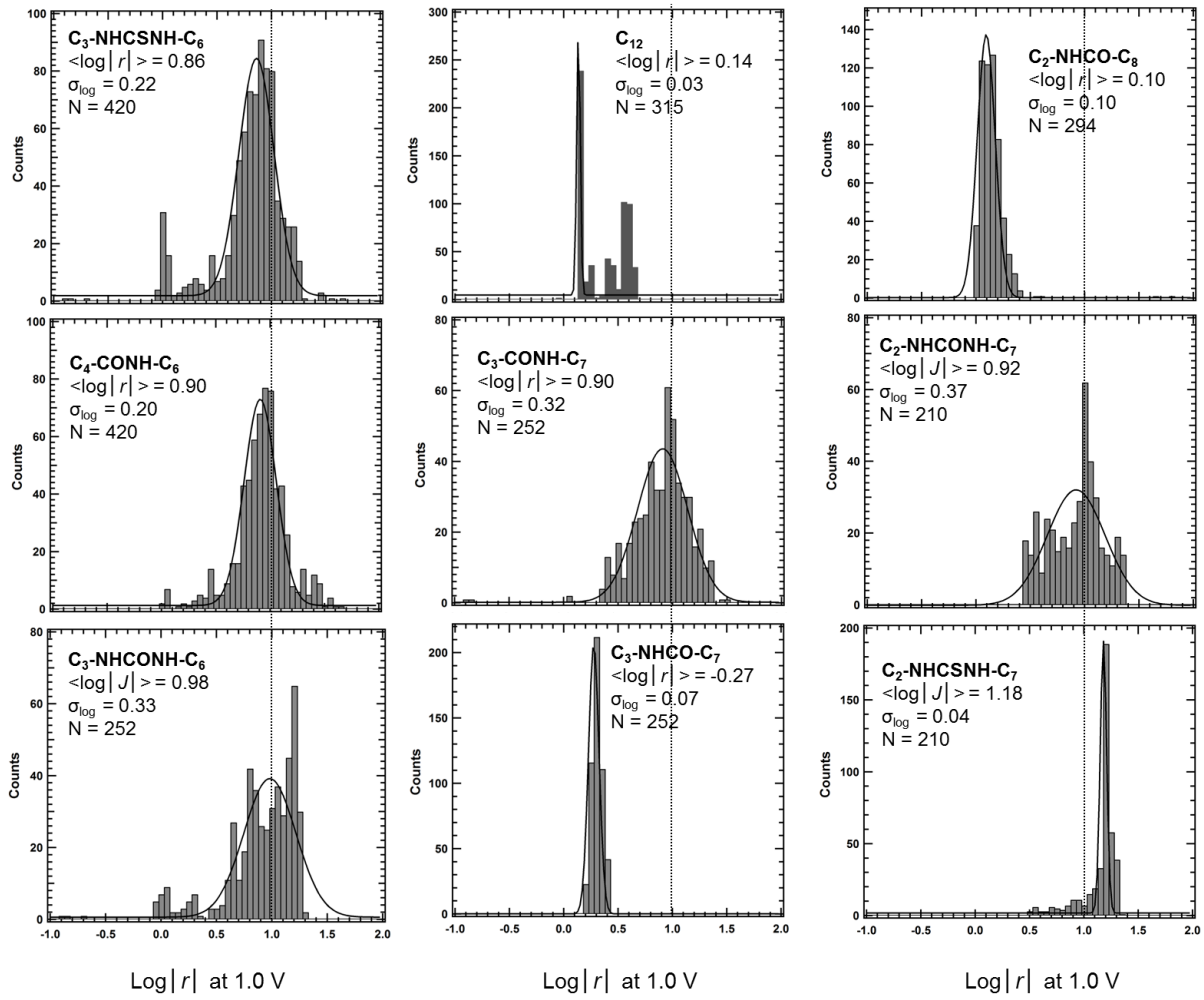

Figure S6. Histograms of the rectification ratio (r^+) at +1.0 V of series II in Figure 1 (N: number of data; $r^+ = \langle|J(+1.0\ V)|/|J(-1.0\ V)|\rangle$; σ: standard deviation of r).

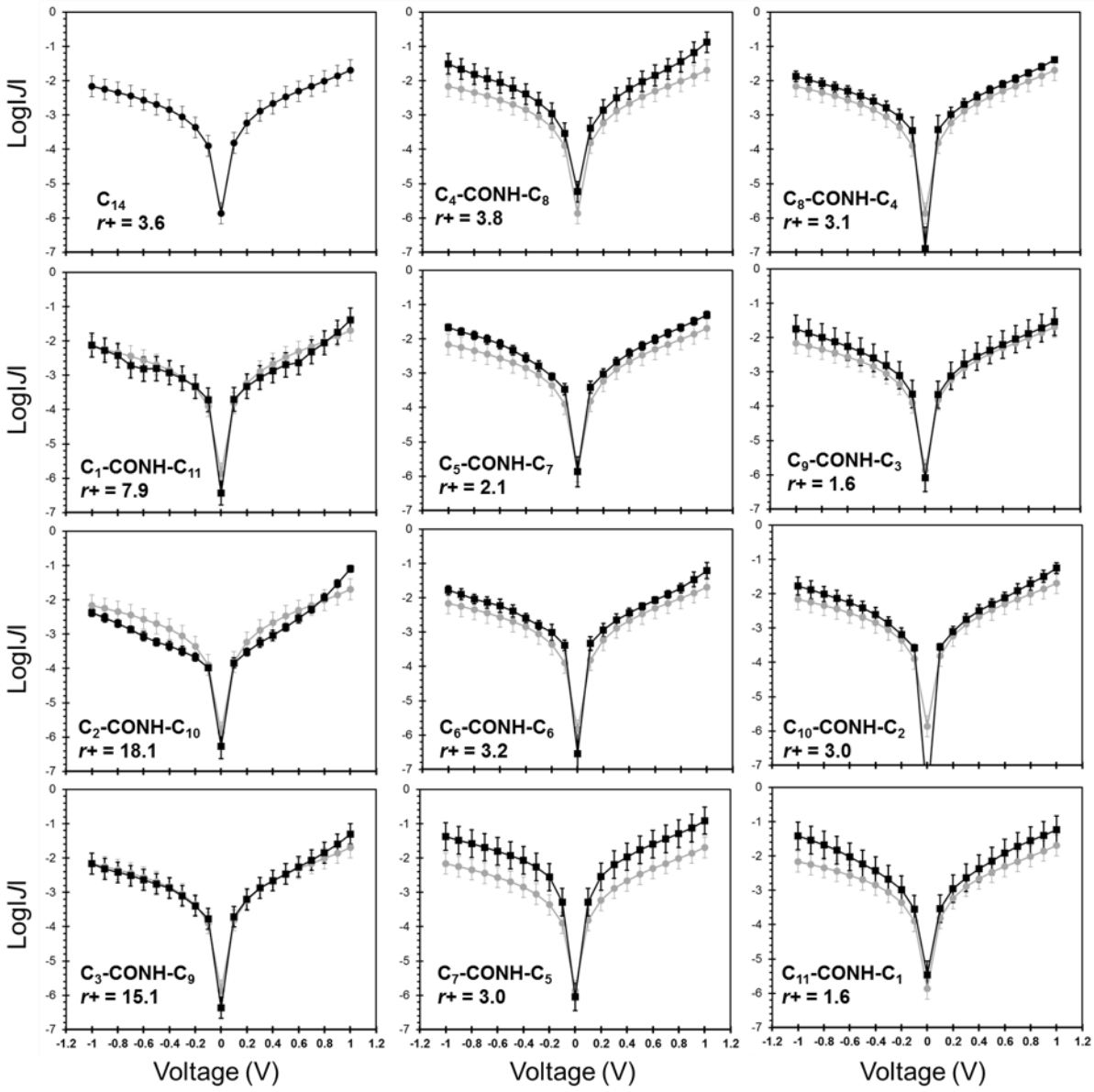

Figure S7. Log|*J*|-*V* plots of SAMs of Series I on Ag^{TS}. For comparison the gray traces in each figure are the log|*J*|-*V* of SAMs of SC_{14} on Ag^{TS}. The error bars represent the standard deviation of the mean values. The value of r^+ represents the rectification ratio at ± 1.0 V.

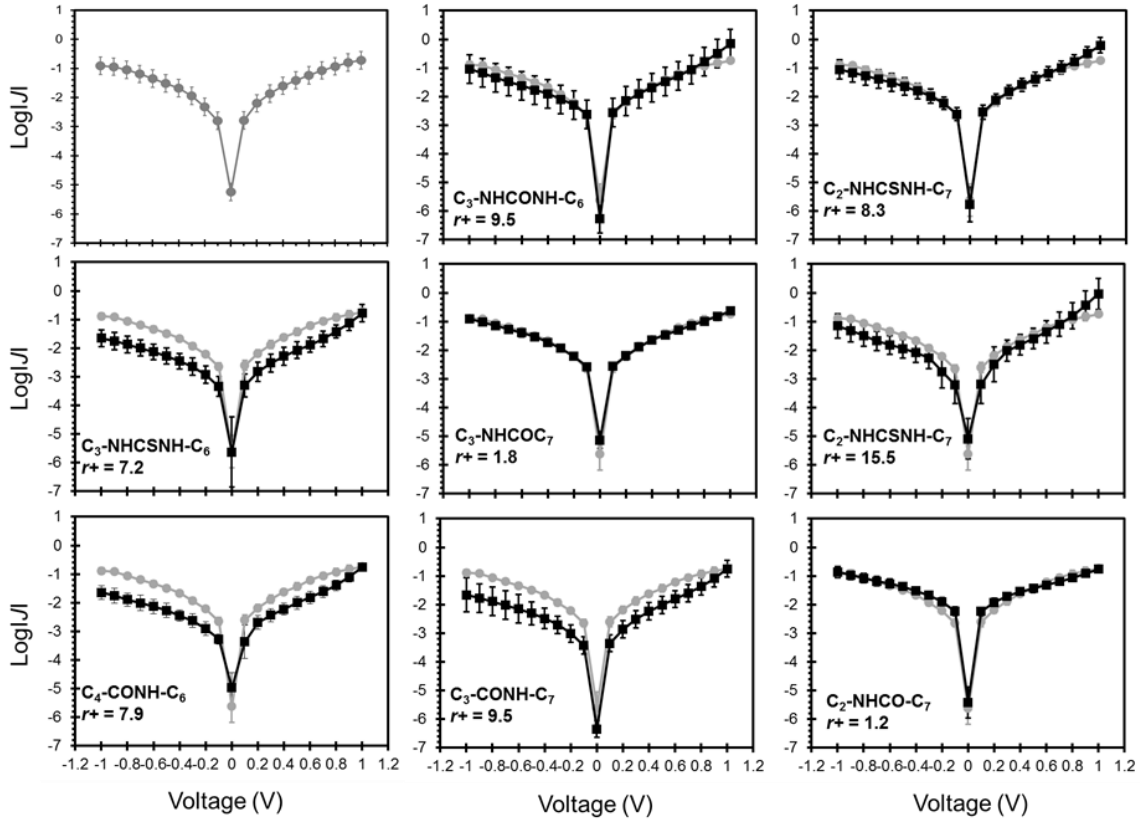

Figure S8. Log|*J*|-*V* plots of SAMs of Series II on Ag^{TS}. For comparison the gray traces are the log|*J*|-*V* of SAMs of SC_{12} on Ag^{TS}. The error bars represent the standard deviation of the mean values. The value of r^+ represents the rectification ratio at ± 1.0 V.

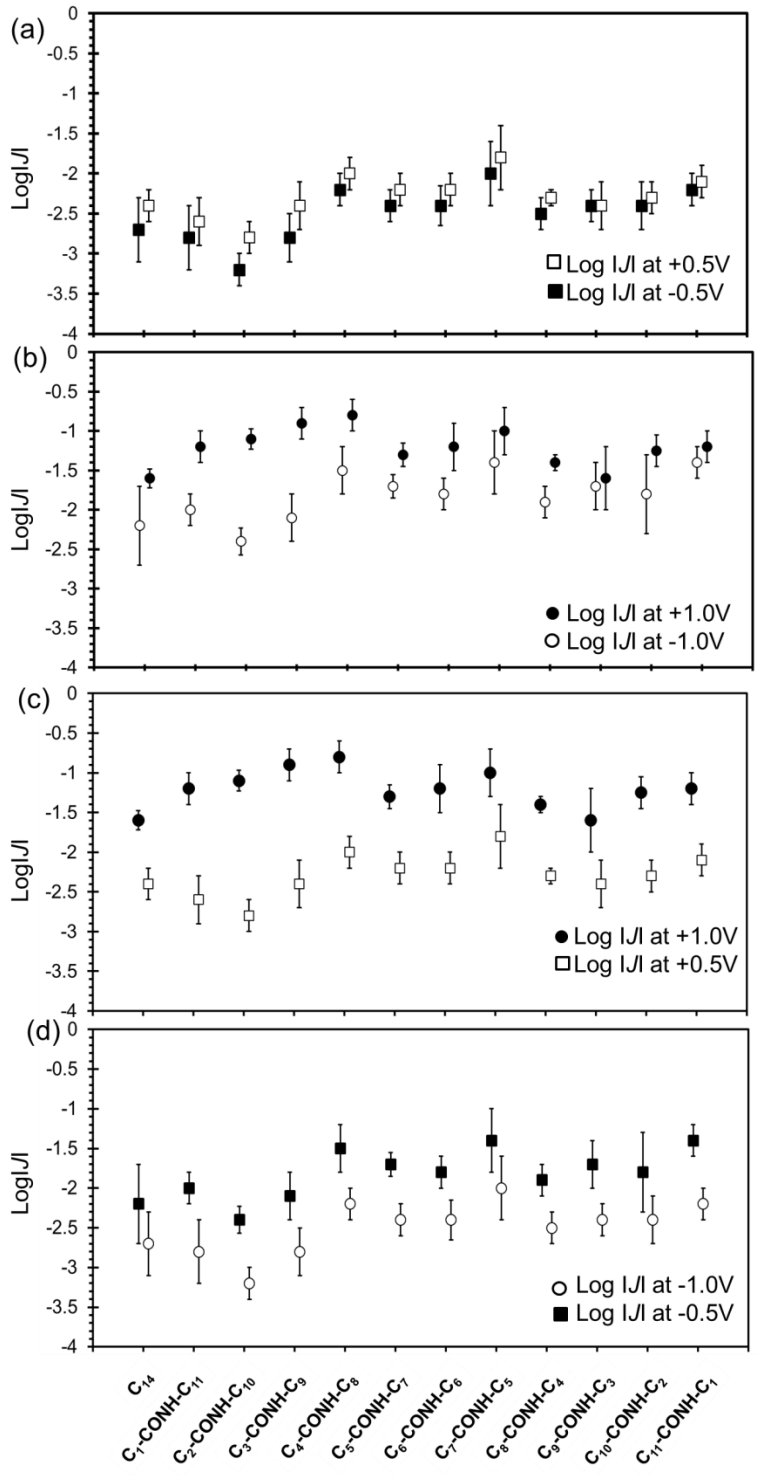

Figure S9. A summary plot of Series I compounds log|*J*| at: a) ± 0.5 V, b) ± 1.0 V, c) +0.5 V and +1.0V and d) -0.5V and -1.0 V. The error bars represent the standard deviation of the mean values (for details of measurements see Supporting Information).

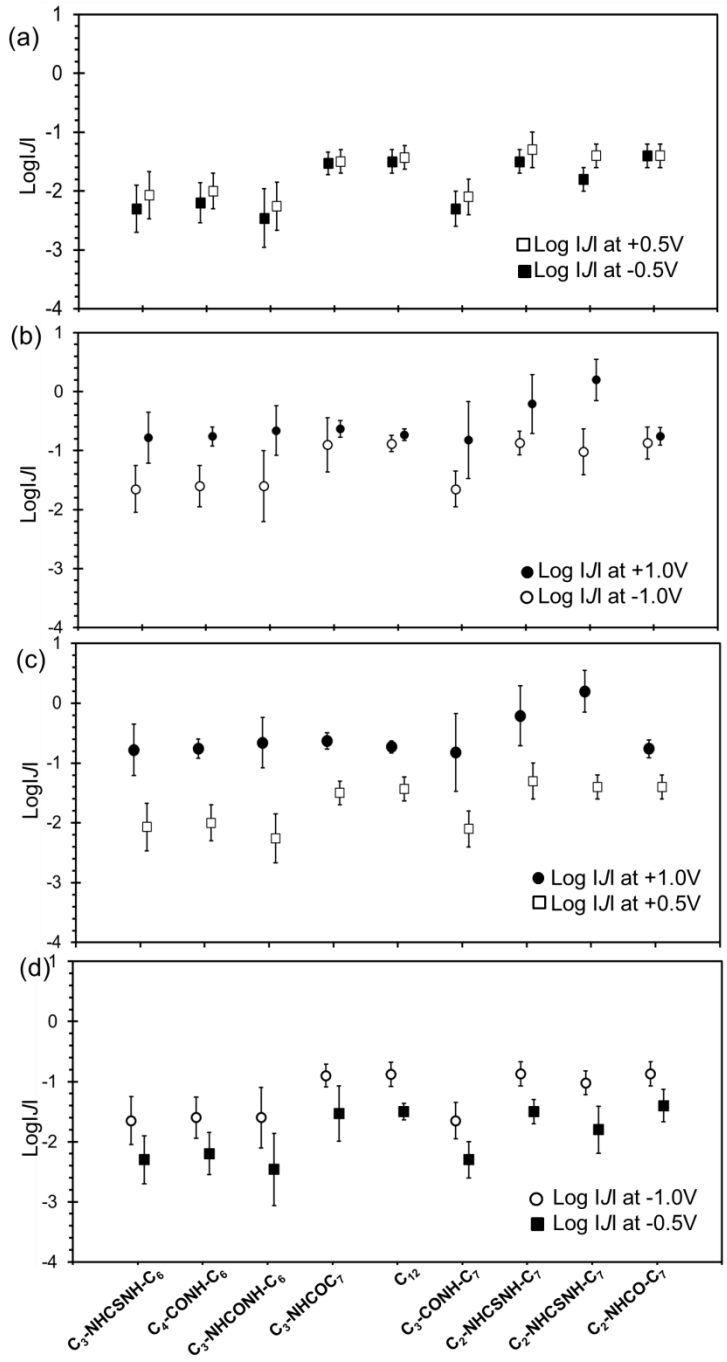

Figure S10. A summary plot of log|*J*| a) at ± 0.5 V, b) at ± 1.0 V, c) at +0.5 V and +1.0V and d) at -0.5V and -1.0 V of Series II compounds. The error bars represent the standard deviation of the mean values (for details of measurements see Supporting Information).

Table S1. Junction performance and rectification ratios observed for SAMs composed of Series II compounds in a Ag/SAM//Ga_2O_3/EGaIn junction.

Compound	+0.5 V		-0.5 V		log|r^+|[a]	σ_{log}	|r^+|
	log|J|	σ_{log}	log|J|	σ_{log}			
C_{14}	-2.4	0.2	-2.7	0.4	0.24	0.13	1.8
C_1-CONH-C_{11}	-2.6	0.3	-2.8	0.4	0.15	0.15	1.5
C_2-CONH-C_{10}	-2.8	0.2	-3.2	0.2	0.39	0.10	2.5
C_3-CONH-C_9	-2.4	0.3	-2.8	0.31	0.29	0.27	2.2
C_4-CONH-C_8	-2.0	0.2	-2.2	0.2	0.17	0.10	1.5
C_5-CONH-C_7	-2.2	0.2	-2.3	0.2	0.11	0.08	1.3
C_6-CONH-C_6	-2.2	0.2	-2.4	0.3	0.19	0.11	1.6
C_7-CONH-C_5	-1.8	0.4	-2.0	0.4	0.17	0.05	1.5
C_8-CONH-C_4	-2.3	0.1	-2.5	0.2	0.22	0.05	1.6
C_9-CONH-C_3	-2.4	0.3	-2.4	0.2	0.05	0.16	1.1
C_{10}-CONH-C_2	-2.3	0.2	-2.4	0.3	0.14	0.12	1.5
C_{11}-CONH-C_1	-2.1	0.2	-2.2	0.2	0.05	0.09	1.1

[a] r^+ = <|J(+0.5 V)|/|J(-0.5 V)|>.

Table S2. Junction performance and rectification ratios observed for SAMs composed of compounds in Series II in a Ag/SAM//Ga_2O_3/EGaIn junction at ±0.5 V.

Compound	**+0.5 V**		**-0.5 V**		**log|r^+|**[a]	**σ_{log}**	**|r^+|**
	log|J|	**σ_{log}**	**log|J|**	**σ_{log}**			
C_3-NHCSNH-C_6	-2.1	0.4	-2.3	0.4	0.08	0.04	1.2
C_4-CONH-C_6	-2.0	0.3	-2.3	0.3	0.21	0.10	1.6
C_3-NHCONH-C_6	-2.3	0.4	-2.5	0.5	0.19	0.20	1.6
C_3-NHCO-C_7	-1.5	0.2	-1.5	0.2	0.19	0.14	1.6
C_{12}	-1.4	0.2	-1.5	0.2	0.16	0.20	1.4
C_3-CONH-C_7	-2.1	0.3	-2.3	0.2	0.19	0.14	1.6
C_2-NHCONH-C_7	-1.3	0.2	-1.5	0.2	0.20	0.11	1.6
C_2-NHCO-C_8	-1.4	0.2	-1.4	0.1	0.00	0.06	1.0
C_2-NHCSNH-C_7	-1.4	0.2	-1.8	0.2	0.36	0.09	2.3

[a] r^+ = <|J(+0.5 V)|/|J(-0.5 V)|>.

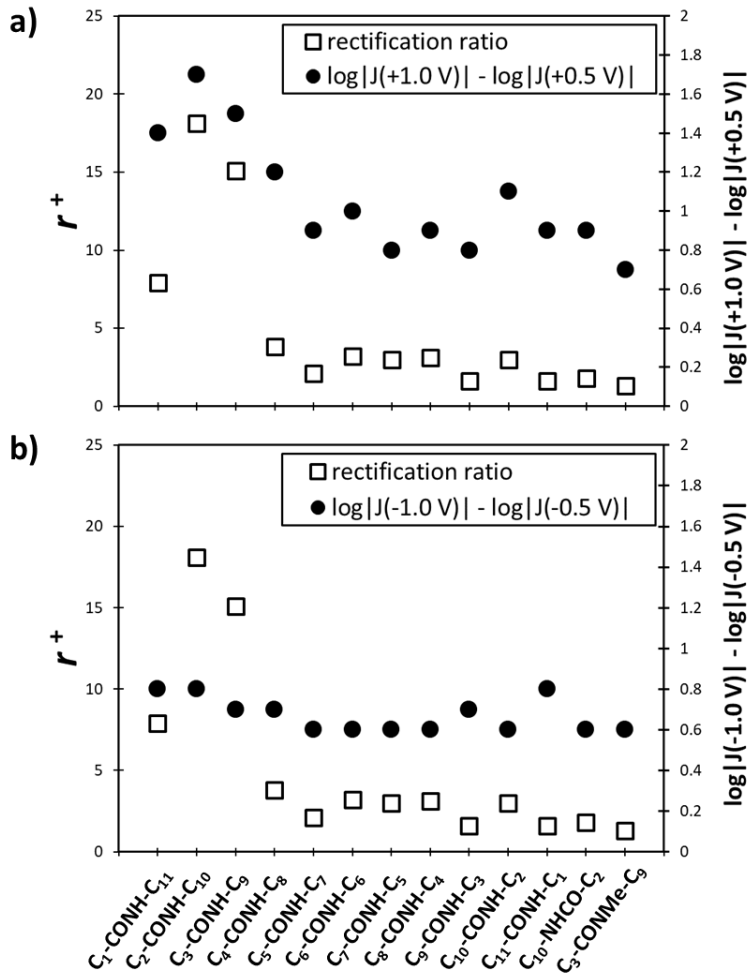

Figure S11. Trend in rectification ratio (empty squares) and the difference in log|*J*| between +0.5 V and +1.0 V (solid circles) at positive bias (**a**) and at negative bias (**b**) for the compounds in Series I.

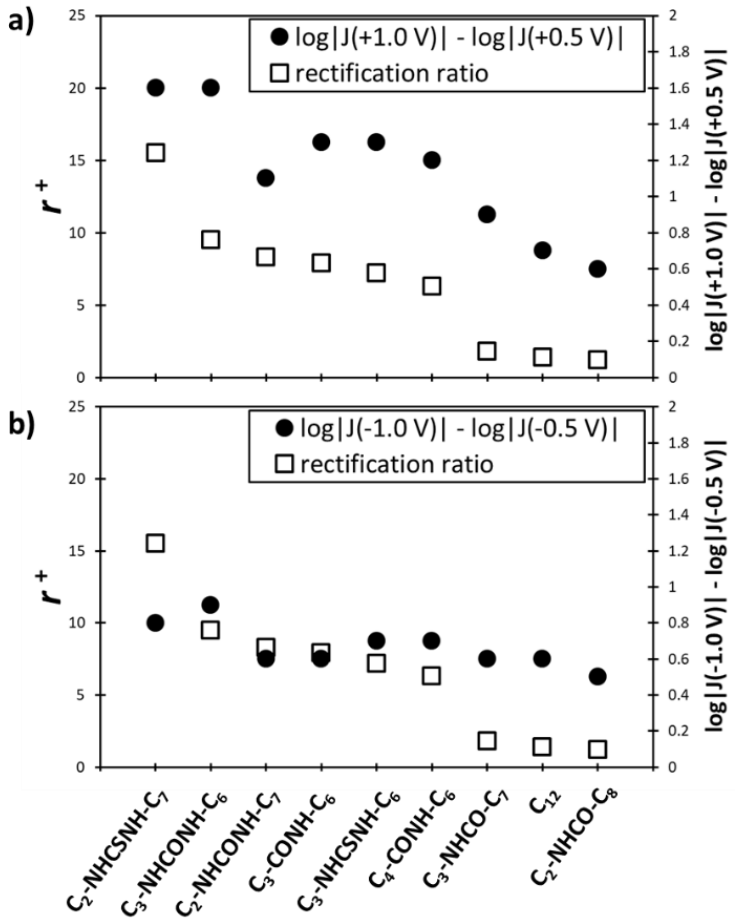

Figure S12. Trend in rectification ratio (empty squares) and the difference in log|*J*| between 0.5 V and 1.0 V (solid circles) at positive bias (**a**) and at negative bias (**b**), for the compounds in Series II.

Trends in log|*J*| at ±0.5 V. The study of rectification in tunneling is one that is least complicated by artifacts, since the same junction is used to make the two critical measurements (at opposite polarities). It is more challenging, technically, to compare the current densities of different molecules because the measurements being compared are performed on different samples/junctions (it is for this reason that we average at least 882 *J*(V) traces). Based on the error in our measurements, we do not attribute small differences in current densities to the electronic structure of the molecules. Trends in log|*J*|, however, are sometimes observed although we are not sufficiently confident in the precision of our measurements to draw conclusions from them. For instance, in this work we state that differences in current densities for Series I, measured at ±0.5 V, are not distinguishable from a C_{14}-alkanethiol, and that current densities for Series II are indistinguishable from a C_{12}-alkanethiol. Nevertheless, we observe a trend when comparing rectifying amides and non-rectifying amides, that we believe may be statistically significant. This trend, shown in Figures S13 and S14, suggests that rectifying amides have lower current densities than non-rectifying amides. (This trend is also observed at ±1.0 V, but is complicated by the emergence of rectification in some molecules and not in others.). These results might suggest that incorporating polar functional groups into alkanethiol-based SAMs *does* influence the shape of the tunneling barrier; polar functional groups decrease the effective tunneling barrier, unless they are within four methylene units of the covalently bound electrode, at which point they increase the tunneling barrier.

Thus, changes in molecular composition may influence the shape of the tunneling barrier—even in cases where they appear not to—but the effects on tunneling current are small, and lie within (or close to) the experimental error associated with our measurements.

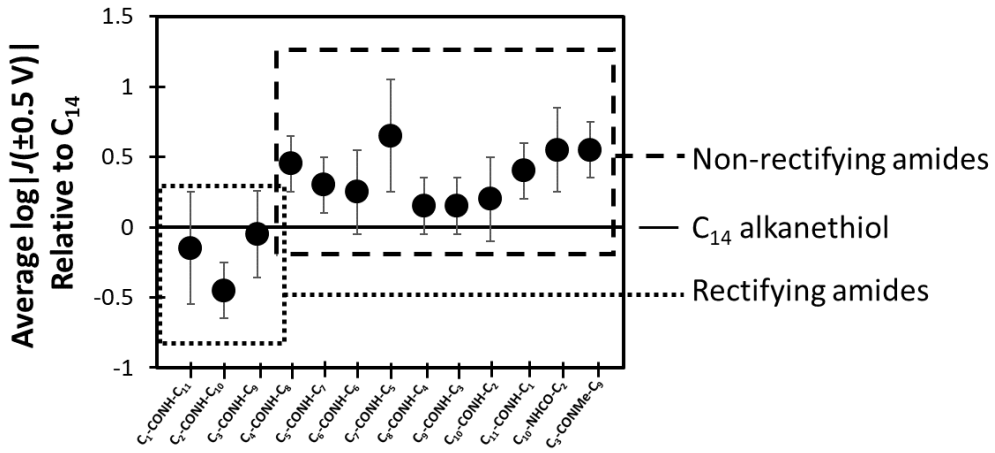

Figure S13. Average value of log|J(±0.5V)| for amides in Series I, relative to C_{14}-alkanethiol.

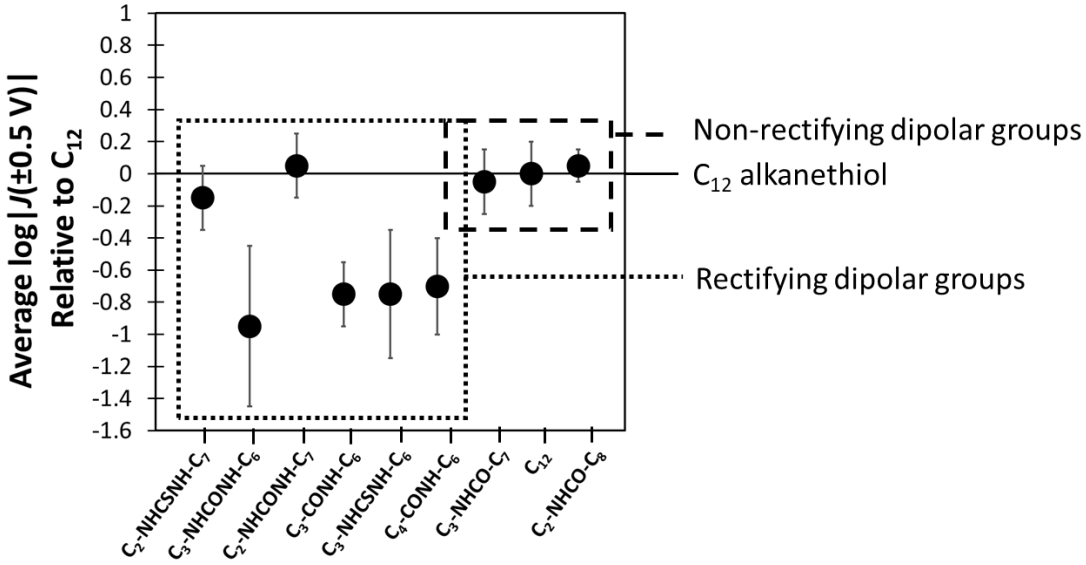

Figure S14. Average value of log|J(±0.5V)| for amides in Series II, relative to C_{14}-alkanethiol.

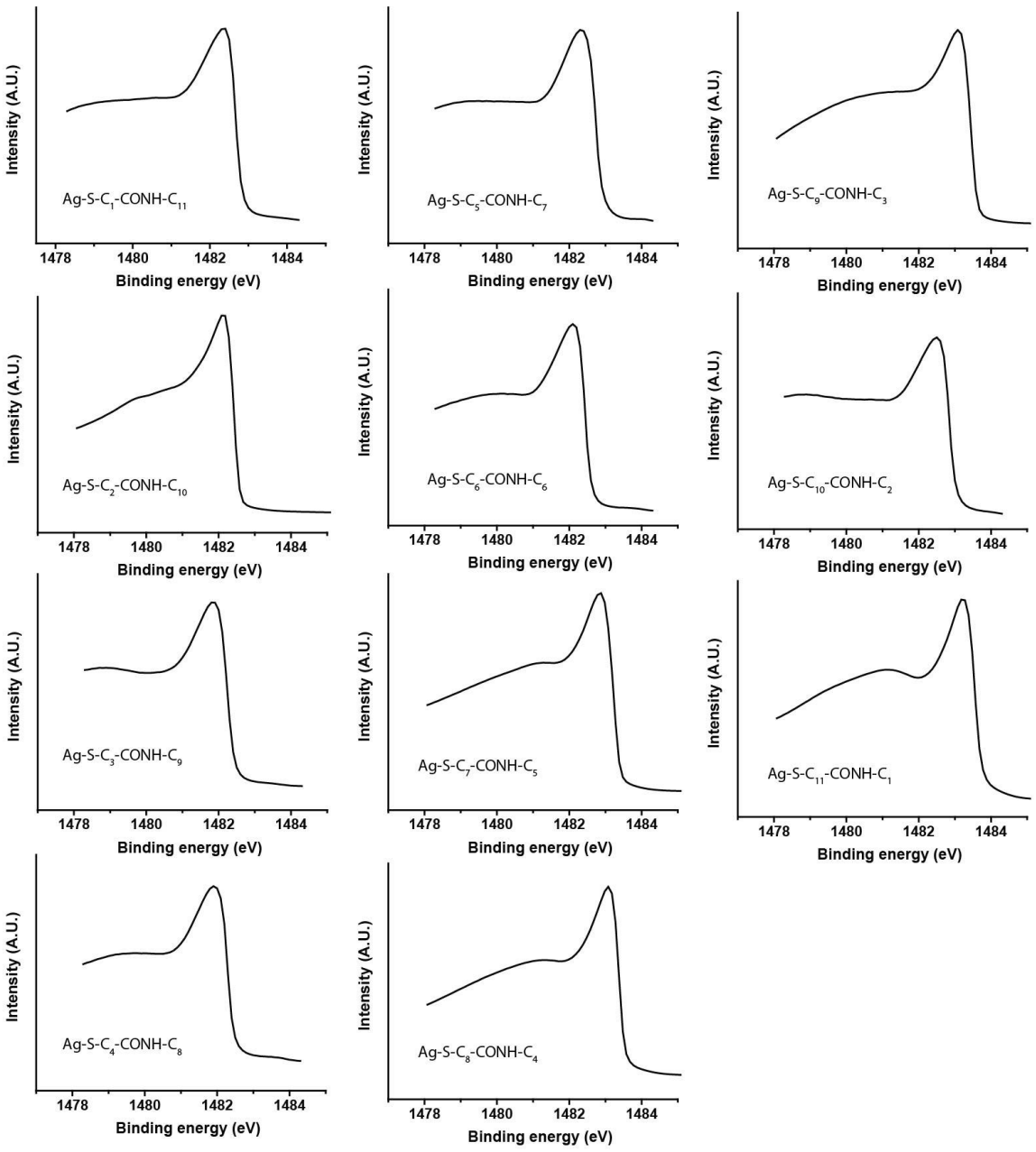

Figure S15. Secondary electron cut-off spectra of SAM series I formed on Ag^{TS} substrates.

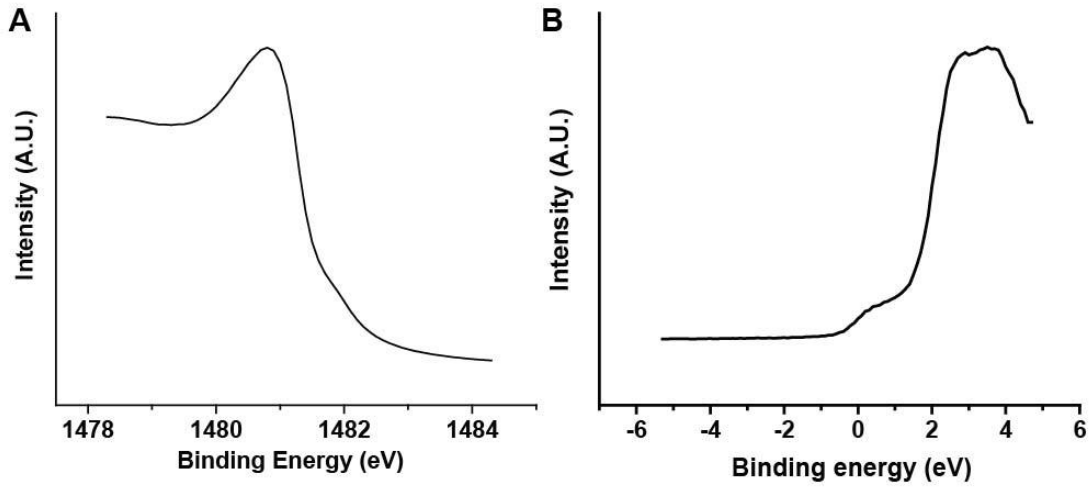

Figure S16. Secondary electron cut-off (A) and Fermi-edge (B) spectra of a sputter cleaned Au substrate. The measured work function of the bare Au surface is 5.1 eV.

Synthetic Procedures.

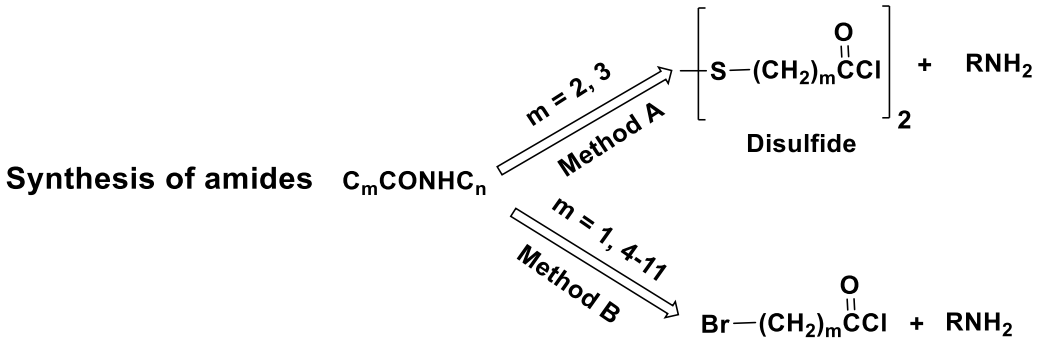

Scheme S1. Synthetic scheme describing the preparation amides from different precursors.

Typical procedure for the synthesis of C_2CONHC_{10} (Method A).

3,3'-Disulfanediyldipropanoic acid (**1**) (2 mmol, 420 mg) was added to 20 mL of anhydrous benzene in a round-bottomed flask. Thionyl chloride (40 mmol, 3 mL) was added to the solution. The mixture was stirred for 12 h under reflux condition, and then concentrated by rotary evaporation. The crude residue, containing compound **2**, was used directly in the next step. Decylamine (4 mmol, 0.8 mL) and triethylamine (8 mmol, 1.1 mL) in 20 mL of anhydrous CH_2Cl_2 was added dropwise to a 20-mL CH_2Cl_2 solution of **2** (from step 1) at 0^oC. The resulting solution was warmed to room temperature and stirred for 3 h. The reaction solution was filtered, and the solid residue was washed with cold CH_2Cl_2 (3 × 10 mL) and recrystallized from ethanol to give compound **3**. Compound **3** (0.4 mmol, 100 mg) was dissolved in 50 mL of MeOH, followed by addition of a solution of tris(2-carboxyethyl)phosphine (TCEP) (250 mg, 1 mmol) in water (2 mL) and 2 mL of aqueous $NaHCO_3$ (3M). The mixture was allowed to stir under a nitrogen atmosphere for 5 hours. Water (20 mL) was then added to the mixture and the solution was extracted with CH_2Cl_2 (3 × 30 mL). The combined organic layer was dried ($MgSO_4$) and evaporated under vacuum to produce the thiol 16 as a white solid in quantitative yield. ^{1}H NMR (500 MHz, $CDCl_3$, 25°C, TMS): δ 5.61 (brs, 1H, NH), 3.27 (q, J = 6.5 Hz, 2H), 2.82 (q, J = 6.5

Hz, 2H), 2.48 (t, *J* = 6.5 Hz, 2H), 1.61 (t, *J* = 6.5 Hz, 1H), 1.50 (m, 2H), 1.38-1.26 (m, 14H), 0.88 (t, *J* = 6.5 Hz, 3H, CH_3) ppm. ^{13}C NMR (125 MHz, $CDCl_3$, 25°C, TMS): δ = 170.5, 40.5, 39.6, 31.9, 29.6, 29.5, 29.3, 29.2, 26.9, 22.6, 20.5, 14.1 ppm. HRMS (ES) calculated for $C_{13}H_{27}NOS$ $(MH)^+$: 246.1892; found: 246.1926.

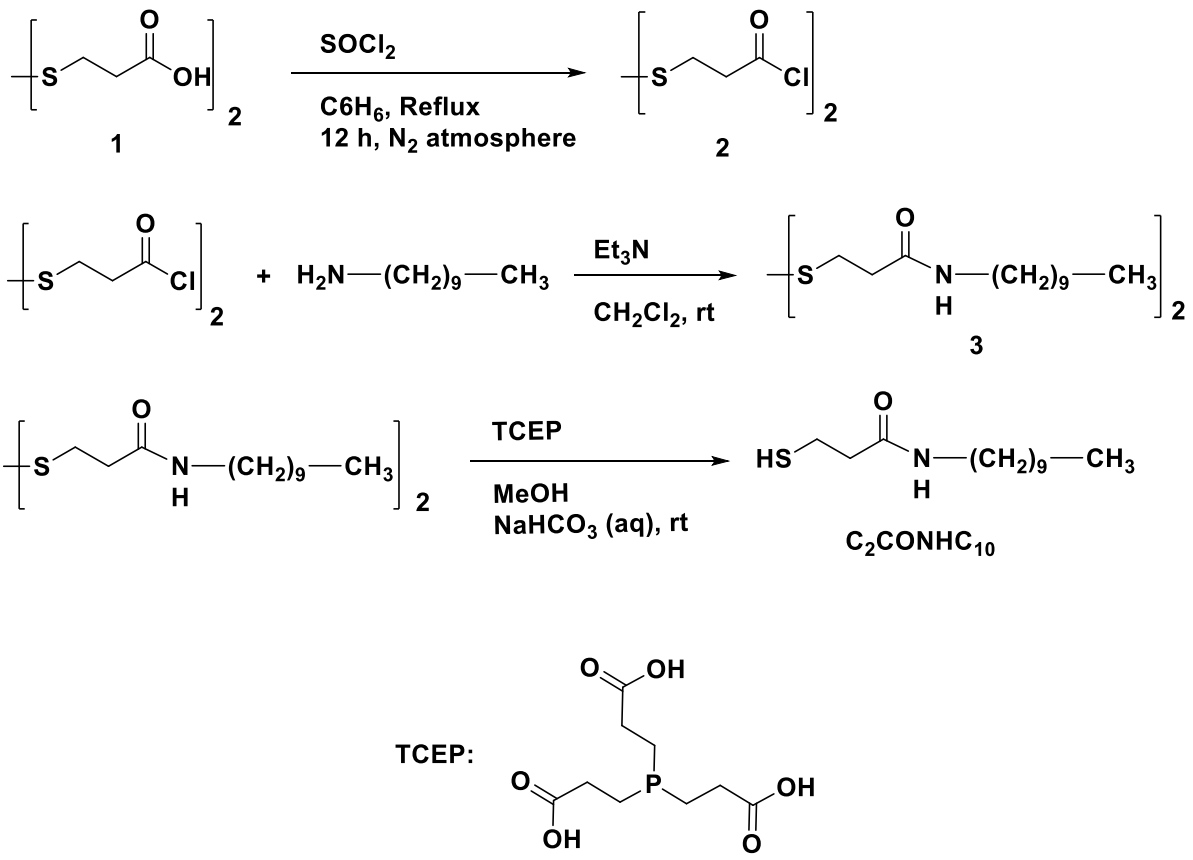

Scheme S2. Synthesis of C_2CONHC_{10}

Typical procedure for the synthesis of C_5CONHC_7 (Method B). Hepthylamine (575 mg, 5 mmol) and triethylamine (1.1 mL, 8 mmol) in 10 mL of CH_2Cl_2 was added dropwise to a 20-mL CH_2Cl_2 solution of 6-bromohexanoyl chloride (852 mg, 4 mmol) at room temperature and stirred for 3 hrs. The reaction solution was then concentrated *in vacuo*, dissolved in CH_2Cl_2 and washed with water. The combined organic layer was dried over anhydrous Na_2SO_4, filtered to separate solids, and concentrated *in vacuo*. Without further purification, the crude compound was

dissolved in 20 mL of EtOH, followed by addition of thiourea (465 mg, 6 mmol). The resulting mixture was refluxed for 4 hrs. After removal of the ethanol *in vacuo*, sodium hydroxide (or potassium hydroxide) (160 mg, 4 mmol) in 20 mL of degassed water was added to the crude mixture (the water was degassed by purging the solution for 10 min with a mild stream of N_2). The reaction mixture was refluxed for 30 min under a N_2 atmosphere (Caution: longer reaction times might cause oxidation of thiol to disulfide). Using an ice bath, the solution was immediately cooled to room temperature and extracted with CH_2Cl_2. The combined organic layer was dried over anhydrous Na_2SO_4, filtered, and concentrated *in vacuo*. The product was usually pure when analyzed by ^{1}H NMR. (500 MHz, $CDCl_3$, 25°C, TMS): δ 3.21 (q, *J* = 8.0 Hz, 2H, CH_2), 2.52 (q, *J* = 8.0 Hz, 2H, C*H*$_2$SH), 2.15 (t, *J* = 7.5 Hz, 2H), 1.65-1.58 (m, 4H), 1.48-1.26 (m, 13H), 0.86 (t, *J* = 6.5 Hz, 3H, CH_3) ppm. HRMS (ES) calculated for $C_{13}H_{27}NOS\ (MH)^+$: 246.1892; found: 246.1914.

Synthesis of $C_{10}NHCOC_2$.

*Step 1, Synthesis of Compound **6***. 325 mg of 10-aminodecan-1-ol (1.88 mmol) was dissolved in 20 mL dichloromethane and cooled to 0 °C. Trimethylamine (0.34 mL, 2.44 mmol) was added drop-wise, followed by the drop-wise addition of propionic anhydride (0.312 mL, 2.44 mmol). The reaction was allowed to warm to room temperature and stirred for 20 hours. The reaction mixture was then transferred to a separatory funnel where it was washed once with H_2O and once with 1M HCl. The organic layer was dried over $MgSO_4$ and concentrated *in vacuo* to afford a white solid (1.70 mmol, 90% yield. ^{1}H-NMR (300 MHz, $CDCl_3$): δ = 5.43 (bs, 1H), 3.63 (t, *J*= 6.6 Hz, 2H), 3.25 – 3.21 (q, *J* = 6.9 Hz, 2H), 2.51 – 2.46 (q, *J* = 7.5 Hz 2H), 2.21 – 2.16 (q, *J* = 7.6 Hz, 2H) 1.58 – 1.53 (m, 2H), 1.51 – 1.45 (m, 2H), 1.28 (s, 10H) 1.19 – 1.15 (m,

3H). ^{13}C-NMR (100 MHz, $CDCl_3$): δ =173.7, 63.0, 39.5, 32.8, 29.8, 29.6, 29.4, 29.4, 29.3, 29.2, 26.8, 25.7, 9.9. HRMS (ESI): m/z calcd for $C_{27}H_{41}N_4$ $[M+H^+]^+$: 230.2115, found: 230.2146.

Step 2, Synthesis of Compound ***7***. 198 mg of compound **6** (0.86 mmol) was dissolved in 8 mL of dichloromethane. 300 mg of triphenylphosphine (1.73 mmol) was then added and the reaction was cooled to 0 °C. A solution of CBr_4 (573.7 mg, 1.73 mmol) in dichloromethane (8 mL) was then added, drop-wise. The reaction was allowed to warm to room temperature and stir for 3 h hours. The reaction mixture was then transferred to a separatory funnel where it was washed twice with H_2O and once with brine. The organic layer was dried over $MgSO_4$ and concentrated *in vacuo* to afford a light yellow oil. The product (**7**) was purified by silica gel column chromatography (4:1, hexane: ethyl acetate) to afford a white solid (0.52 mmol, 60% yield). ^{1}H-NMR (500 MHz, $CDCl_3$): δ = 5.40 (bs, 1H), 3.44 – 3.40 (m, 2H), 3.28 – 3.23 (m, 2H), 2.23 – 2.18 (m, 2H), 1.90 – 1.83 (m, 2H) 1.53 – 1.48 (m, 2H), 1.45 – 1.40 (m, 2H), 1.30 (bs, 10H), 1.19 – 1.15 (m, 3H). HRMS (ESI): m/z calcd for $C_{27}H_{41}N_4$ $[M+H^+]^+$: 292.1271, found: 292.1266.

Step 3, Synthesis of $C_{10}NHCOC_2$. 125 mg of **7** (0.43 mmol) and 65.5 mg of thiourea (0.86 mmol) were dissolved in 5mL anhydrous ethanol. The reaction was refluxed for 12 hours. The reaction was then cooled to room temperature and the solvent removed *in vacuo*. To the resulting oil was added 1.1 eq. of KOH, dissolved in 5 mL degassed H_2O. The reaction mixture was refluxed for 30 minutes, at which time it was allowed to cool to room temperature and neutralized with dilute HBr. The product was extracted twice with 10 mL dichloromethane, dried over $MgSO_4$ and concentrated *in vacuo* to afford a white solid. (0.37 mmol, 85% yield). ^{1}H-NMR (500 MHz, $CDCl_3$): δ = 5.40 (bs, 1H), 3.28 – 3.24 (q, *J*= 6.84 Hz, 2H), 2.69 (t, *J* = 7.2 Hz, 2H), 2.23 – 2.19 (q, *J* = 7.6 Hz 2H), 1.71 – 1.64 (m, *J* = 7.2 Hz, 2H) 1.53 – 1.48 (m, 2H), 1.40 –

1.36 (m, 2H), 1.28 (s, 10H), 1.17 (t, J = 7.7 Hz,3H).^{13}C-NMR (100 MHz, $CDCl_3$): δ = 174.1, 39.5, 39.2, 29.8, 29.7, 29.5, 29.4, 29.4, 29.3, 29.2, 28.5, 26.9, 9.7. HRMS (ESI): m/z calcd for $C_{27}H_{41}N_4$ $[M+H^+]^+$: 246.1886, found: 246.1890.

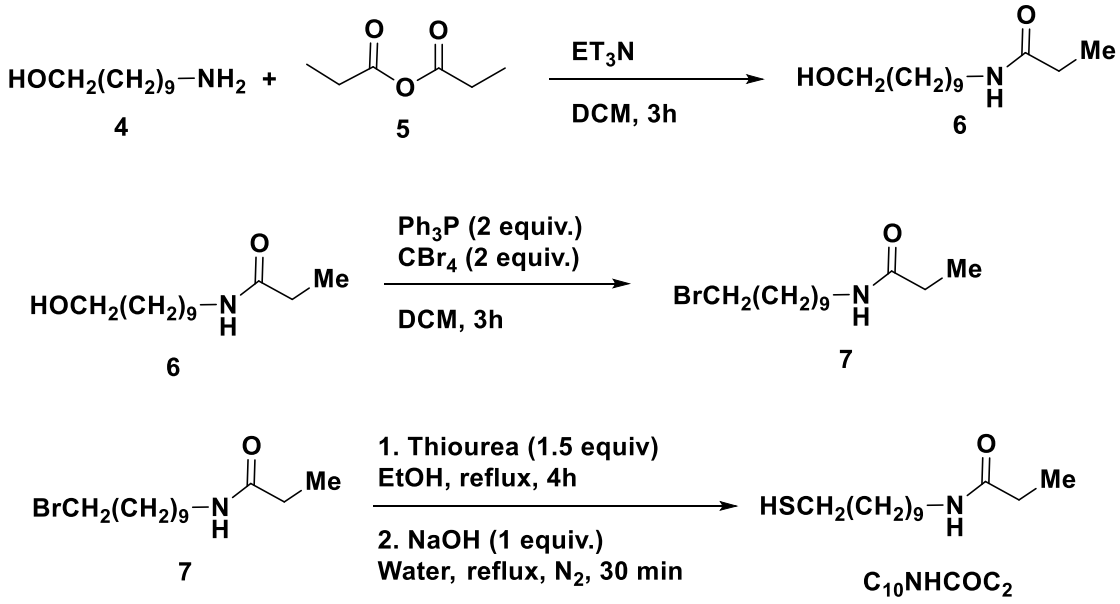

Scheme S3. Synthesis of $C_{10}NHCOC_2$

Synthesis of urea and thiourea containing alkylthiolates. The synthesis begins with diamino-disulfides that are either coupled to an alkyl amine with triphosgene to form the urea, or with the alkyl isothiocyanate to yield the thioureas. Once purified, the disulfides are reduced to the corresponding thiol with tris(2-carboxyethyl)phosphine hydrochloride (TCEP) in quantitative yields. The formation of the disulfide precursor provides a convenient synthetic strategy, since the disulfides are easier to purify and have a longer shelf life than the corresponding thiols. Synthesis and purification of the amide-containing compounds was achieved following a previously published procedure.[6]

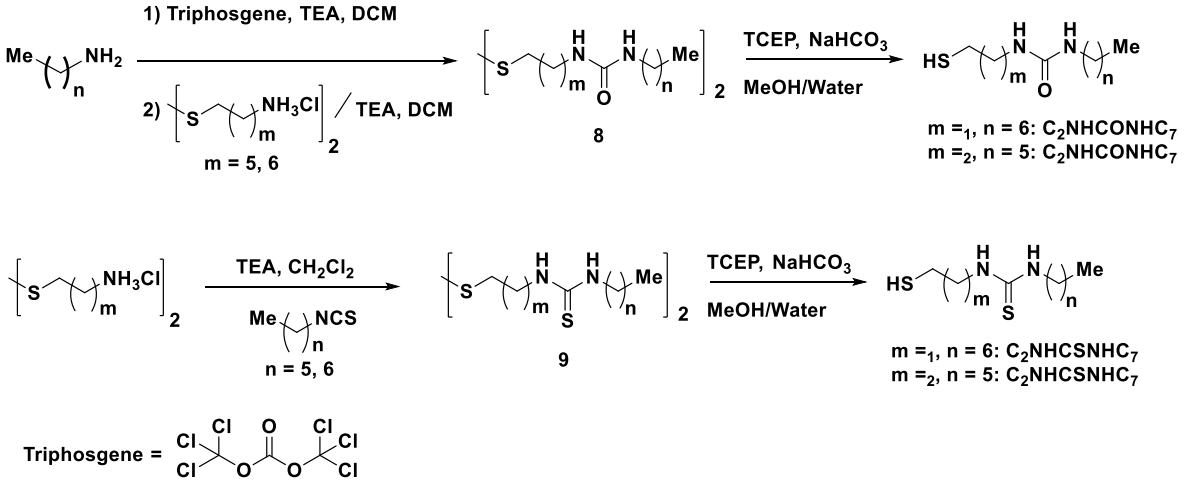

Scheme S4. Synthetic scheme describing the preparation of ureas and thioureas.

Typical procedure for the preparation of urea-containing alkylthiolates. A solution of the heptylamine (1.0 g, 8.7 mmol) and triethylamine (0.88 g, 8.7 mmol) in CH_2Cl_2 (20 mL) was added dropwise to a stirred ice-cooled solution of triphosgene (0.86 g, 0.29 mmol) in CH_2Cl_2 (20 mL) over a period of 15 mins. The ice-bath was removed and the mixture was allowed to stir at room temperature for another 30 mins. The mixture was cooled again in an ice-bath and solid cystamine dihydrochloride (0.98 g, 4.35 mmol) was added at once followed by a solution of triethylamine (1.76 g, 17.4 mmol) in CH_2Cl_2 (20 mL) added dropwise over a period of 15 mins. The ice-bath was removed and the mixture was allowed to stir at room temperature for 5 hours. The precipitated solid was filtered, washed with dilute HCl solution and water, and dried under vacuum. The collected solid was purified by recrystallization from ethanol to produce the compound **8** as a colorless solid (1.6 g, 84 %). ^{1}H NMR (300 MHz, DMSO-d_6): δ 6.03 (t, J = 6.1 Hz, 2H), 5.95 (t, J = 6.3 Hz, 2H), 3.25 (q, J = 6.5 Hz, 4H), 2.93 (q, J = 6.3 Hz, 4H), 2.70 (t, J = 6.7 Hz, 4H), 1.30 (m, 4H), 1.22 (br s, 16 H), 1.22 (t, J = 6.5 Hz, 6H) ppm. Compound **8** (50 mg, 0.11 mmol) was then dissolved in methanol (50 mL) and a solution of TCEP (35 mg, 0.14 mmol) in water (2 mL) was added and the mixture was allowed to stir under

nitrogen atmosphere for 5 hours. Water (20 mL) was then added to the mixture and the solution was extracted with CH_2Cl_2 (3 x 20 mL). The combined organic layer was dried over $MgSO_4$, filtered, and evaporated under vacuum to produce the thiol as a white solid in quantitative yield. ^{1}H NMR (300 MHz, $CDCl_3$): δ 3.39 (t, *J* = 5.8 Hz, 2H), 2.16 (t, *J* = 7.0 Hz, 2H), 2.70 (q, *J* = 7.6 Hz, 2H), 1.51 (m, 2H), 1.38-1.26 (m, 9H), 1.22 (t, *J* = 6.5 Hz, 3H) ppm. HRMS (ES) calculated for $C_{10}H_{23}N_2OS$ $(MH)^+$: 219.1531; found: 219.1545; calculated for $C_{10}H_{22}N_2OSNa$ $(MNa)^+$: 241.1351; found: 241.1367.

Typical procedure for the preparation of thiourea-containing alkylthiolates. Solid cystamine dihydrochloride (1.0 g, 4.4 mmol) was as added at once to an ice-cold solution of isothiocyanate (1.4 g, 8.8 mmol) in CH_2Cl_2 (20 mL) followed by a solution of triethylamine (0.88 g, 8.8 mmol) in CH_2Cl_2 (20 mL) added dropwise over a period of 15 mins. The ice-bath was removed and the mixture was allowed to stir at room temperature for 5 hours. The mixture was then washed with dilute HCl solution (1 x 15 mL), water (1 x 15 mL), and brine solution (1 x 15 mL). The organic mixture was then dried and evaporated under vacuum to yield a beige solid that was purified by recrystallization (twice) from ethyl acetate/hexane mixture to produce a colorless precipitate of compound **9** (1.43 g, 70 %). ^{1}H NMR (300 MHz, $CDCl_3$): δ 6.45 (br s, 2H), 6.24 (br s, 2H), 3.93 (q, *J*= 5.9 Hz, 4H), 3.37 (br s, 4H), 2.99 (t, *J*= 6.4 Hz, 4H), 1.60 (q, *J*= 7.0 Hz, 4H), 1.32 (m, 16H), 0.88 (t, *J*= 7.0 Hz, 6H) ppm. HRMS (ES) calculated for $C_{20}H_{43}N_4S_4$ $(MH)^+$: 467.2365; found: 467.2374; calculated for $C_{20}H_{43}N_4S_4Na$ $(MNa)^+$: 489.2185; found: 489.2199. Compound **9** (50 mg, 0.11 mmol) was then dissolved in methanol (50 mL) and a solution of tris(2-carboxyethyl)phosphine) (TCEP) (35 mg, 0.14 mmol) in water (2 mL) was added and the mixture was allowed to stir under nitrogen atmosphere for 5 hours. Water (20 mL) was then added to the mixture and the solution was extracted with CH_2Cl_2 (3 x 20 mL). The combined

organic layer was dried over $MgSO_4$, filtered, and evaporated under vacuum to produce the thiol as an oily residue that solidifies upon cooling (quantitative yield). ^{1}H NMR (300 MHz, $CDCl_3$): δ 5.96 (br s, 1H), 5.86 (br s, 1H), 3.79 (q, *J*= 6.5 Hz, 2H), 3.29 (br s, 2H), 2.81 (q, *J*= 5.9 Hz, 2H), 1.61 (q, *J*= 7.6 Hz, 2H), 1.42-1.28 (m, 9H), 0.89 (t, *J*= 6.5 Hz, 3H) ppm.

References

1. Barber, J. R., Yoon, Hyo Jae, Bowers, Carleen M., Thuo, Martin M., Breiten, Benjamin, Gooding, Diana M., Whitesides, George M., The Influence of Environmental Factors on the Measurement of Rates of Charge Transport across Ag^{TS}/SAM//Ga_2O_3/EGaIn Junctions. *Chem. Mater.* **2014**, *26*, 3938.
2. Simeone, F. C.; Yoon, H. J.; Thuo, M. M.; Barber, J. R.; Smith, B.; Whitesides, G. M., Defining the Value of Injection Current and Effective Electrical Contact Area for EGaIn-Based Molecular Tunneling Junctions. *J. Am. Chem. Soc.* **2013**, 18131.
3. Bowers, C. M., Liao, K.C., Yoon, H.J., Rappoport, D., Baghbanzadeh, M., Simeone, F.C, Whitesides, G.M., Introducing Ionic and/or Hydrogen Bonds into the SAM//Ga2O3 Top-Interface of Ag^{TS}/$S(CH_2)_nT$//Ga_2O_3/EGaIn Junctions. *Nano Lett.* **2014**, *14*, 3521.
4. Rothemund, P.; Morris Bowers, C.; Suo, Z.; Whitesides, G. M., Influence of the Contact Area on the Current Density across Molecular Tunneling Junctions Measured with EGaIn Top-Electrodes. *Chem Mater* **2018**, *30*, 129.
5. Weiss, E. A.; Kaufman, G. K.; Kriebel, J. K.; Li, Z.; Schalek, R.; Whitesides, G. M., Si/SiO2-templated formation of ultraflat metal surfaces on glass, polymer, and solder supports: their use as substrates for self-assembled monolayers. *Langmuir* **2007**, *23*, 9686.
6. Thuo, M. M.; Reus, W. F.; Simeone, F. C.; Kim, C.; Schulz, M. D.; Yoon, H. J.; Whitesides, G. M., Replacing -CH2CH2- with -CONH- Does Not Significantly Change Rates of Charge Transport through Ag-TS-SAM//Ga2O3/EGaIn Junctions. *J. Am. Chem. Soc.* **2012**, *134*, 10876.
7. Love, J. C.; Estroff, L. A.; Kriebel, J. K.; Nuzzo, R. G.; Whitesides, G. M., Self-assembled monolayers of thiolates on metals as a form of nanotechnology. *Chem. Rev.* **2005**, *105*, 1103.